

2. Thermonuclear Reactions

$10^7 - 10^9 \text{ K}$

$1 \text{ keV} - 100 \text{ GeV}$

General properties

nuclear radius $R = R_0 A^{1/3}_{14} \quad R_0 = 1,2 \text{ fm}$

nuclear density $\rho = 2,3 \cdot 10^3 \frac{\text{g}}{\text{cm}^3} = 0,14 \frac{\text{amu}}{\text{fm}^3}$

Weizsäcker mass formula

$$M(A, z) = z m(^1\text{H}) + (A-z)m_n - B.E./c^2$$

$$c^2 = 931,5 \text{ MeV}$$

total binding energy

$$B.E. = a_v A$$

$$a_v = 15.5 \text{ MeV} \quad \text{volume term}$$

$$- a_s A^{2/3} \quad a_s = 16.8 \text{ MeV} \quad \text{surface term}$$

$$- a_c z(z-1) A^{-1/3} \quad a_c = 0.72 \text{ MeV} \quad \text{Coulomb term}$$

$$- a_{\text{sym}} \frac{(A-2z)^2}{A} \quad a_{\text{sym}} = 23 \text{ MeV} \quad \text{symmetry term}$$

$$+ \frac{1 + (-1)^A}{2} (-1)^z a_p A^{-3/4} \quad a_p = 34 \text{ MeV} \quad \text{pairing term}$$

nuclear shell model

Maria Goeppert Mayer Nobel Prize 1963

each nucleon moves in spherically symmetric mean potential $V(r)$

Woods Saxon potential

$$V(r) = - \frac{V_0}{1 + \exp\left(\frac{r-R}{a}\right)}$$

angular momentum ℓ

spin s

total angular momentum j

$$j^2 = (\ell + s)^2 = \ell^2 + 2\ell s + s^2$$

$$\Rightarrow \ell-s = \frac{1}{2}(j^2 - \ell^2 - s^2)$$

quantum mechanical expectation value

$$\langle \ell-s \rangle = \frac{1}{2} [j(j+1) - \ell(\ell+1) - s(s+1)]$$

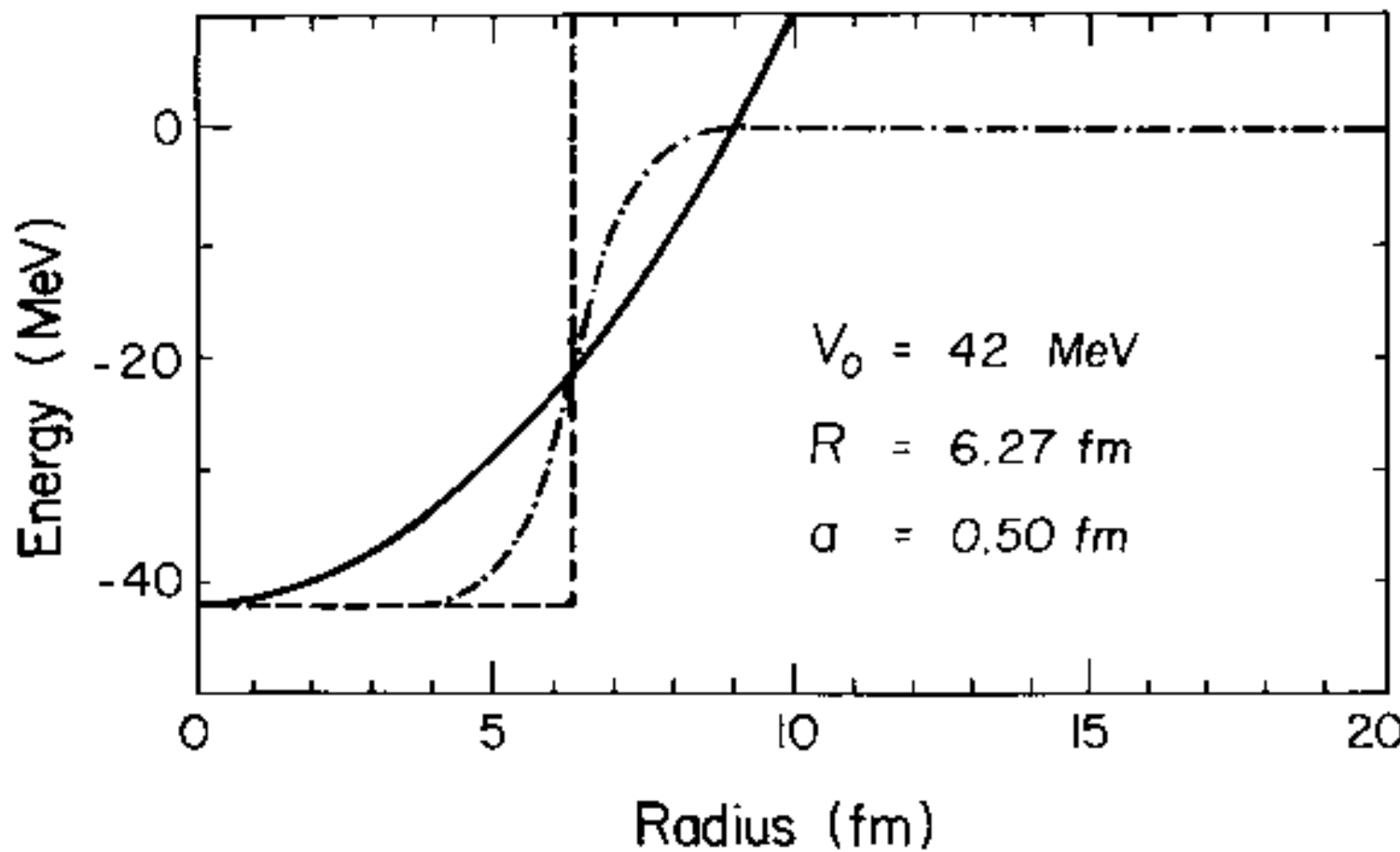


Fig. 2.1. Approximate potentials for the nuclear shell model. The solid curve represents the 3-dimensional harmonic oscillator potential, the dashed curve the infinite square well and the dot-dashed curve a more nearly realistic Woods-Saxon potential, $V(r) = -V_0/[1 + \exp\{(r - R)/a\}]$ (Woods & Saxon 1954). Adapted from Cowley (1995).

spin-orbit potential, splitting increases with ℓ

$$\langle \ell \cdot s \rangle_{\ell+\frac{1}{2}} - \langle \ell \cdot s \rangle_{\ell-\frac{1}{2}} = \frac{1}{2} (2\ell+1)$$

\Rightarrow magic numbers of shell closures

nuclear reactions

cross section

classical: cross-sectional area of sphere

$$\sigma = \pi (R_1 + R_2)^2 = \pi (1.2 \cdot 10^{-13} (A_1^{\frac{1}{3}} + A_2^{\frac{1}{3}}) \text{ cm})^2$$

$$\sim 10^{-24} \text{ cm}^2 \equiv 1 \text{ barn} \quad \text{unit for cross section}$$

Intermediate form

4s	2
3d	10
2g	18
1i	26
3p	6
2f	14
1h	22
3s	2
2d	10
1g	18
2p	6
1f	14
2s	2
1d	10
1p	6
1s	2

Intermediate form with spin orbit

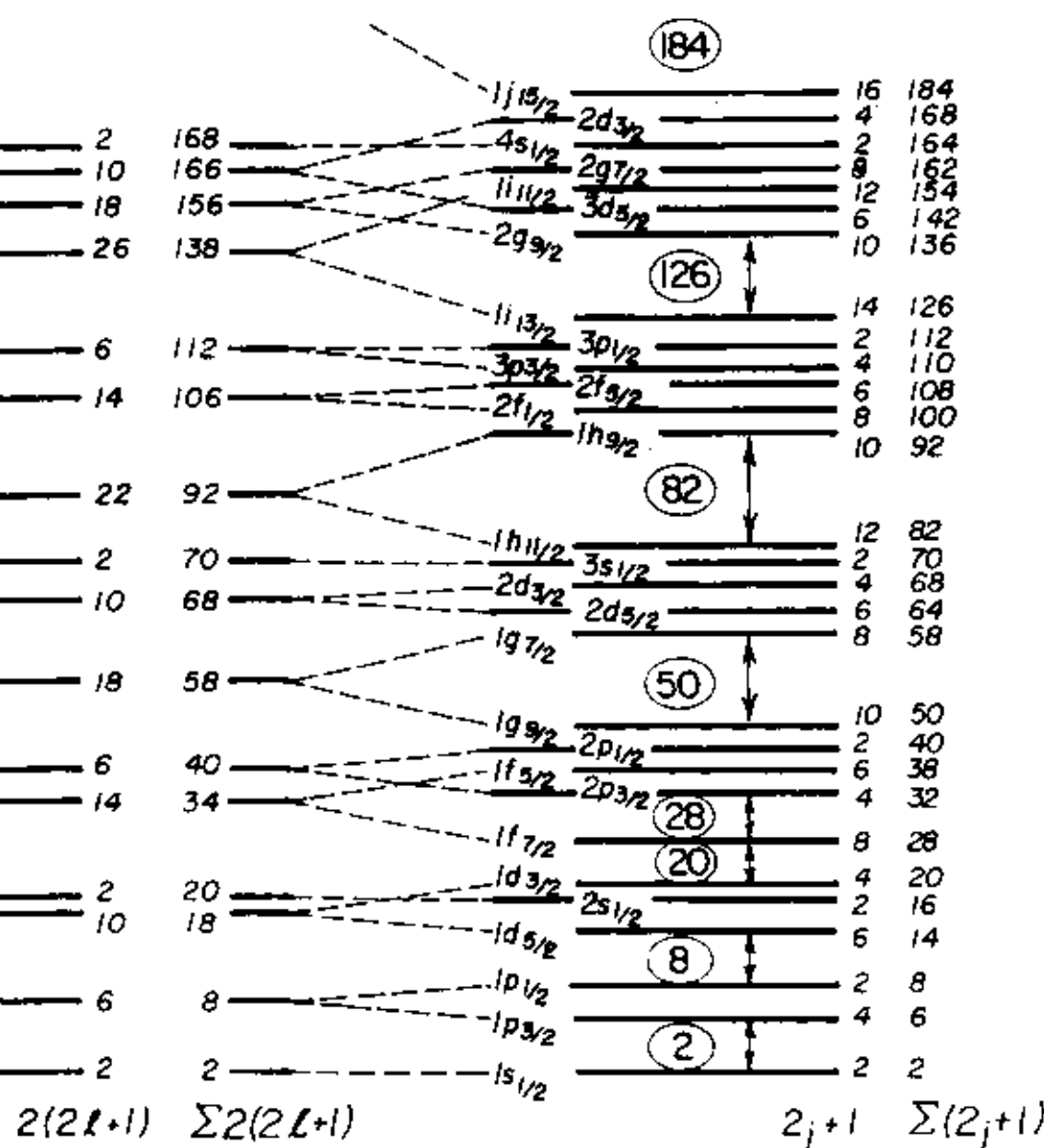


Fig. 2.3. At left, energy levels for a Woods-Saxon potential with $V_0 \simeq 50$ MeV, $R = 1.25A^{1/3}$ fm and $a = 0.524$ fm, neglecting spin-orbit interaction. At right, the same with spin-orbit term included. Adapted from Krane (1987).

Coulomb barrier penetration probabilities

or Gamow factors

particle moving along $-x$ is described by plane wave

$$\Psi = A e^{i(\omega t + kx)} = A e^{\frac{i}{\hbar} (Et + \sqrt{2m(E-V)}x)}$$

total probability of barrier penetration e^{-G}

$$G = \frac{2}{\hbar} \int_a^b \sqrt{2m(V(x)-E)} dx = \frac{2\sqrt{2mE}}{\hbar} \int_a^b \sqrt{\frac{b}{x} - 1} dx$$

$$b = \frac{z_1 z_2 e^2}{E} = \frac{2 z_1 z_2 e^2}{m v^2}$$

the classical turning point

$$G = \frac{4 z_1 z_2 e^2}{\hbar v} \left[\underbrace{\arccos \sqrt{\frac{a}{b}} - \sqrt{\frac{a}{b}} \sqrt{1 - \frac{a}{b}}}_{\approx \frac{\pi}{2}} \right]$$

$a \ll b$

quite insensitive to a

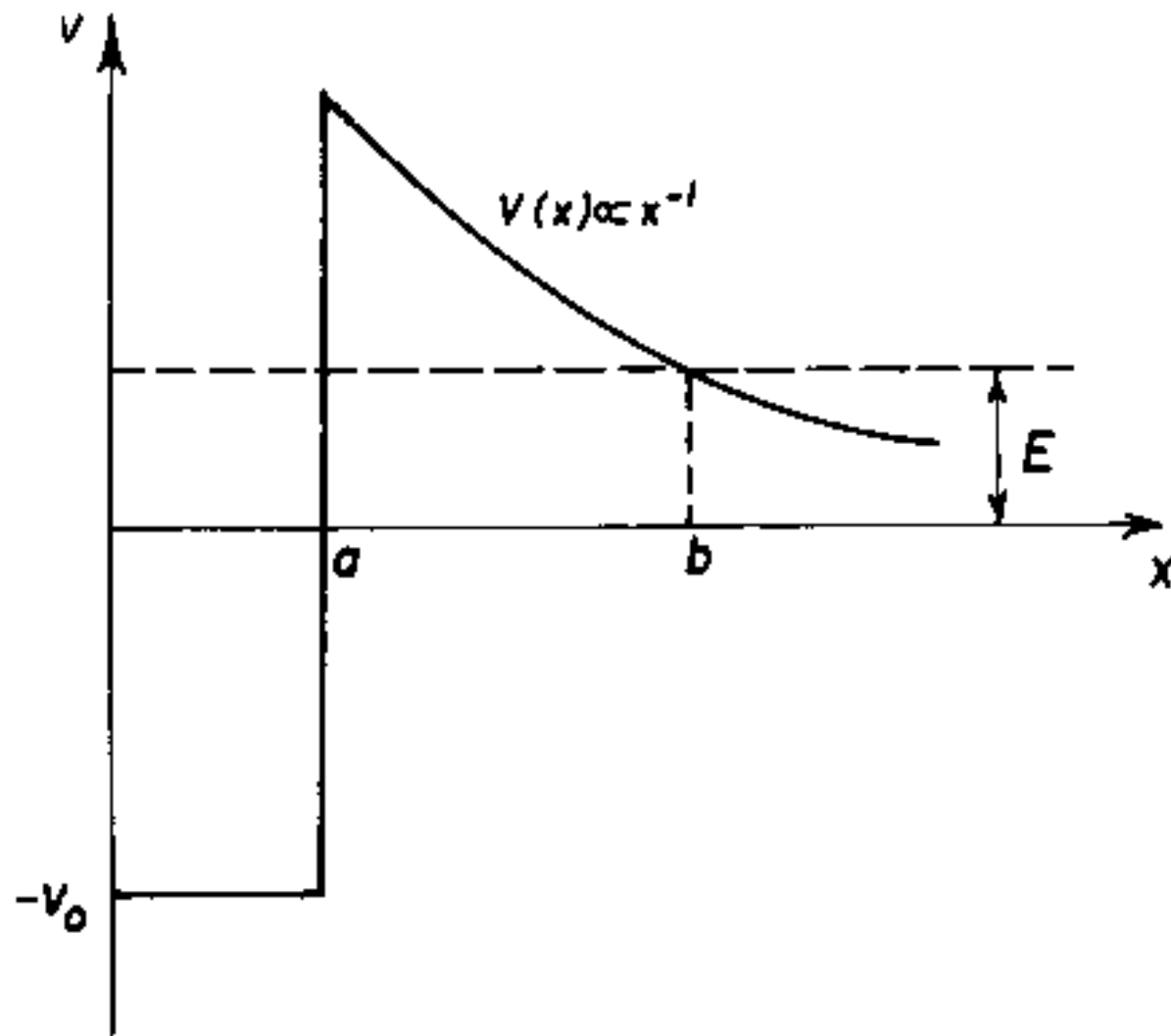


Fig. 2.7. Coulomb barrier penetration by a charged particle. a is the range of the nuclear force and b the classical turning point.

barrier penetration probability for s-waves

$$(II) \quad P \propto e^{-2\pi z_1 z_2 e^2 / \hbar v} \equiv e^{-2\pi \gamma} = e^{-B E^{-1/2}}$$

$$(III) \quad B = \sqrt{2m} \pi z_1 z_2 \frac{e^2}{\hbar} = 31.3 z_1 z_2 \sqrt{\hbar}$$

A reduced mass in amu

E in keV

e.g. 1 keV proton $P \approx 10^{-9}$

The steep dependence of P on energy leads
to the use of the astrophysical s-factor
which contains the purely nuclear part
of the cross section

$$(I) \quad \sigma(E) = \frac{1}{E} e^{-2\pi \gamma} S(E)$$

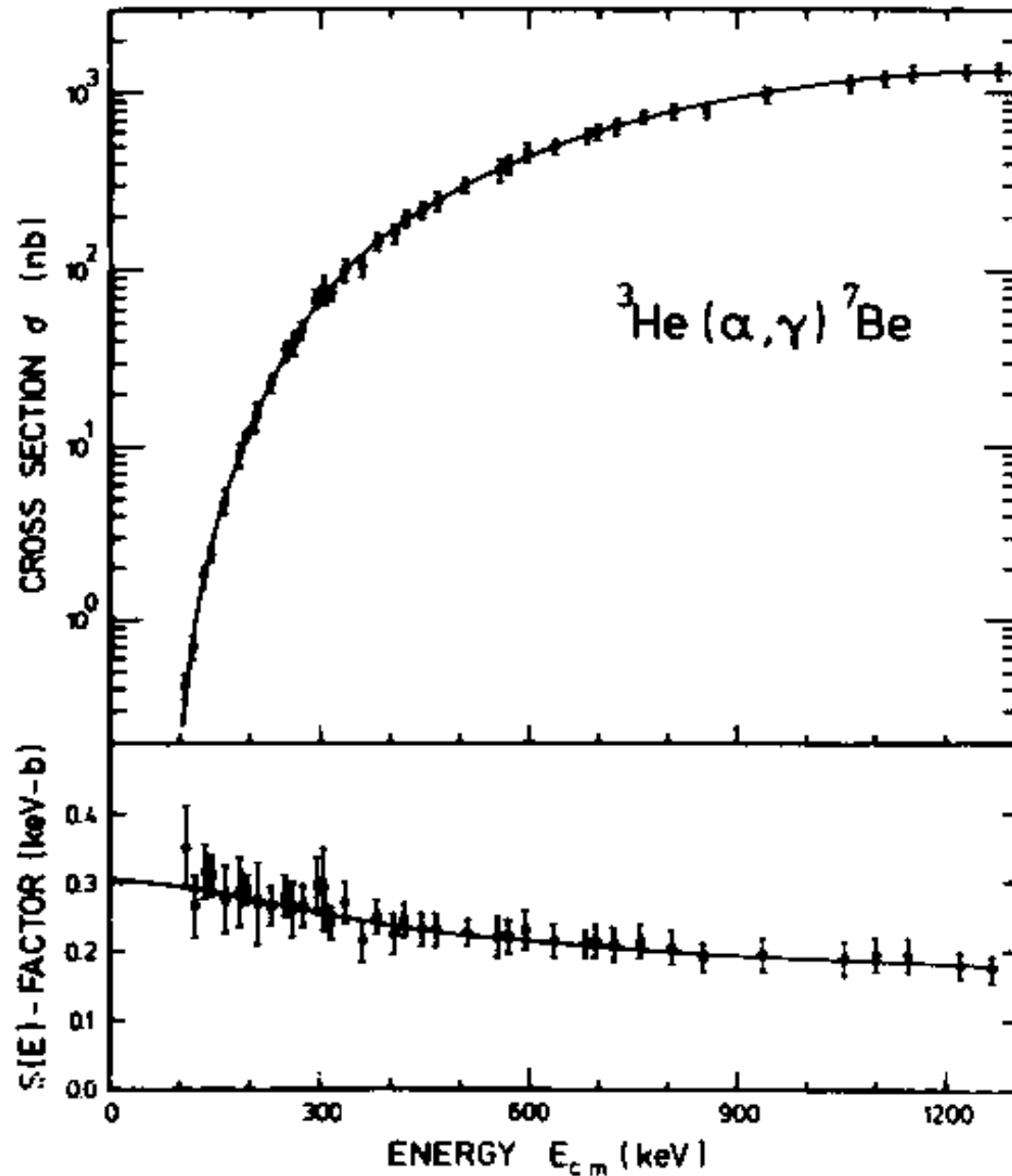


Fig. 2.8. Energy dependence of the cross-section and of $S(E)$ for a typical nuclear reaction. The extrapolation of $S(E)$ to zero energy is carried out with the aid of theory. After Rolfs and Rodney (1988). Copyright by the University of Chicago. Courtesy Claus Rolfs.

A more exact expression for the barrier penetration factor, derived for example by Clayton (1968), is

$$P_\ell(E) = \left(\frac{E_c}{E}\right)^{1/2} \exp\left[-BE^{-1/2} + 4\left(\frac{E_c}{\hbar^2/2mR^2}\right)^{1/2} - 2\left(\ell + \frac{1}{2}\right)^2 \left(\frac{\hbar^2/2mR^2}{E_c}\right)^{1/2}\right] \quad (2.23)$$

or numerically

$$\begin{aligned} P_\ell(E) = & \left(\frac{E_c}{E}\right)^{1/2} \exp[-BE^{-1/2} + 1.05(ARZ_1Z_2)^{1/2} \\ & - 7.62\left(\ell + \frac{1}{2}\right)^2 (ARZ_1Z_2)^{-1/2}] \end{aligned} \quad (2.24)$$

where

$$E_c = \frac{Z_1 Z_2 e^2}{R} = 1.0 \frac{Z_1 Z_2}{A_1^{1/3} + A_2^{1/3}} \text{ MeV} \quad (2.25)$$

is the height of the Coulomb barrier and R is in fm.

laboratory measurements of cross sections
are extrapolated, using s -factors to
energies relevant in stars

Thermonuclear reaction rates

in hot plasma, the reaction rate per unit volume
between particles of types i and j :

$$(VI) \quad \gamma_{ij} = n_i n_j \underbrace{(1 + \delta_{ij})^{-1}}_{\text{in case of identical particles}} \underbrace{\langle \sigma v \rangle_{ij}}_{\text{velocity averaged product of cross-section and rel. velocity}}$$

number density n_i is related to the total mass density ρ

$$n_i = 6.02 \cdot 10^{23} \rho \frac{x_i}{A_i} = 6.02 \cdot 10^{23} \rho Y_i$$

$\rho \left(\frac{\text{g}}{\text{cm}^3} \right)$ X_i abundance by mass fraction

energy production per unit mass

$$\mathcal{E} = (r_{ij} - r_{ji}) \frac{Q}{\rho} - \nu \text{ losses}$$

averaging over the Maxwell distribution

$$\langle \sigma v \rangle = \sqrt{\frac{8}{\pi m}} (kT)^{-3/2} \int_0^\infty E \sigma(E) e^{-E/kT} dE$$

$\sigma(E)$ see (I) varies slowly with energy
→ mean value

$$(V) \quad \langle \sigma v \rangle = \sqrt{\frac{8}{\pi m}} \left(\frac{kT}{h} \right)^3 \langle s(E) \rangle \int_0^{\infty} e^{-\frac{E}{kT} - 2\ln \eta} dE$$

using (II) :

$$(IV) \quad f(E) = e^{-\left(\frac{E}{kT} + B E^{-1/2}\right)} \quad B \text{ see (III)}$$

$f(E)$ has maximum for an energy

$$E_0 = \left(\frac{B k T}{2} \right)^{2/3}$$

$$f(E_0) = e^{-\left(B^2/(kT)\right)^{1/3} \left(2^{1/3} + 2^{-2/3}\right)} = e^{-\frac{3E_0}{kT}} \equiv e^{-\tilde{\tau}}$$

$$\text{and } \tilde{\tau} = 3 \left(\frac{B}{2kT} \right)^{2/3}$$

feature peak

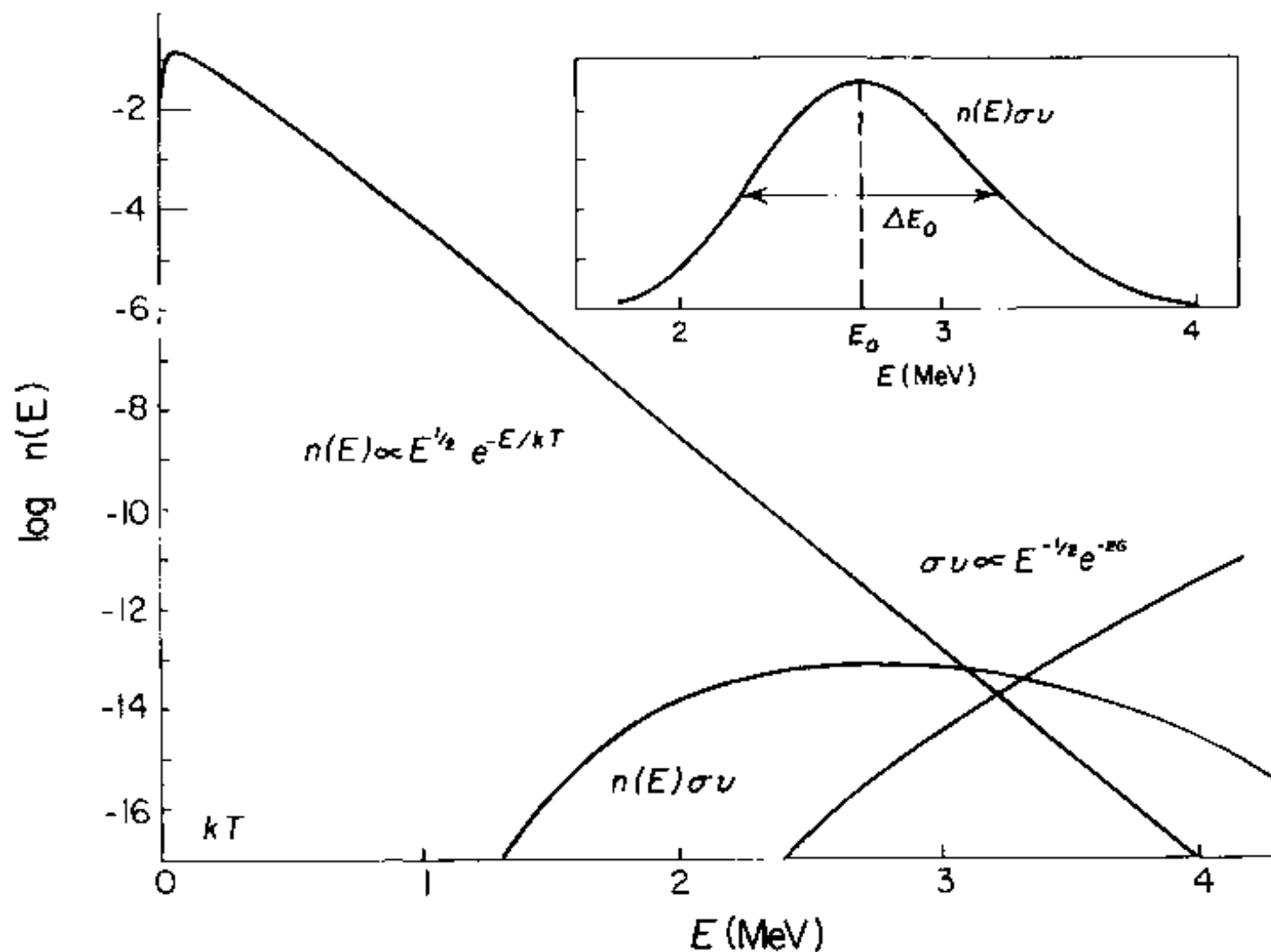


Fig. 2.9. Dependence of particle number and barrier penetration probability on energy for $^{12}\text{C} + ^{12}\text{C}$ at a temperature $kT = 100$ keV. In this case, the energy at the Gamow peak, shown on a linear scale in the inset, is well within the range of typical laboratory energies. Adapted from Krane (1987).

two contrary exponential dependencies in (IV)

→ reaction rates are only significant
for particles in a small range around E_0

$$E_0 \gg kT$$

Resonant reactions

compound nucleus excited level
energy above ground state

$$E_K = E_p + Q$$

projectile energy E close to E_p

be measured in the laboratory. The integral can be approximated by the ‘method of steepest descents’ in which $f(E)$ is approximated by a Gaussian with the same peak value and the same second derivative at that peak, i.e.

$$\int_0^\infty f(E) dE \simeq f(E_0) \sqrt{[2\pi f(E_0)/ - f''(E_0)]} = \frac{2}{3}\pi^{1/2} kT \tau^{1/2} e^{-\tau}. \quad (2.59)$$

Owing to the asymmetry in $f(E)$, the best value to take for $\langle S(E) \rangle$ turns out to be $S(E'_0) \simeq E_0 + \frac{5}{6}kT$ rather than $S(E_0)$. Making all the substitutions in Eq. (2.54) one finds

$$\langle \sigma v \rangle \simeq \frac{8}{81} \frac{\hbar}{\pi Z_1 Z_2 e^2 m} \tau^2 e^{-\tau} S(E'_0) = \frac{7.2 \times 10^{-19}}{AZ_1 Z_2} \tau^2 e^{-\tau} S(E'_0) \text{ cm}^3 \text{ s}^{-1}, \quad (2.60)$$

where $S(E'_0)$ is in keV barns, and

$$\tau = 3E_0/kT = 19.7 (Z_1^2 Z_2^2 A / T_7)^{1/3} \quad (2.61)$$

where T_7 is in units of 10^7 K.

From Eqs. (2.60), (2.61), one can deduce an approximate power-law dependence of specific reaction rates on temperature, T^ν , since

$$\nu \equiv \frac{\partial \log \langle \sigma v \rangle}{\partial \log T} = \frac{\tau - 2}{3}. \quad (2.62)$$

For example, in the interior of the Sun ($T_7 = 1.5$; $kT = 1.3$ keV), one has the following:

Reaction	E_0 (keV)	τ	ν
$p + p$	5.9	13.7	3.9
$p + {}^{14}\text{N}$	27	63	20

These temperature dependences are illustrated in Fig. 5.5.

→ cross section enhanced by resonant effects

excited level broadened, finite lifetime τ

$$P(E) dE = \frac{\Gamma/2\pi}{(E - E_R)^2 + (\Gamma/2)^2} dE$$

$$\Gamma = \frac{t}{\tau} = \Gamma_p + \Gamma_n + \Gamma_\alpha + \Gamma_p - \Gamma_j + \dots$$

total width = sum of partial widths

rate at which excited state is formed

by incoming particles with E_i , $P(E)$

Breit-Wigner formula for single level resonance

$$\sigma(E) = \pi \bar{\lambda}^2 (C_p) (1 - S_{12}) \omega \frac{\Gamma_a \Gamma_b}{(E - E_p)^2 + (\Gamma_b)^2}$$

with $\omega = \frac{2\bar{I}+1}{(2\bar{I}_1+1)(2\bar{I}_2+1)}$

\bar{I} angular momentum of excited state in compound nucleus

$$\bar{I} = I_1 + I_2 + l$$

Γ_a width for elastic resonant scattering

σ maximum for $\Gamma_a = \Gamma_b = \Gamma/2$

neutron capture reactions

no Coulomb barrier

capture rate dominated at $\sim 30 \text{ keV}$ by s-waves

Breit-Wigner formula

$$\sigma_n(E_{\text{nd}}) \propto \bar{\lambda}^2 \Gamma_n \underbrace{\Gamma_x(E_n + Q)}_x$$

$$\text{since } Q \gg E_n \rightarrow \approx \Gamma_x(Q)$$

independent of energy

x refers to γ or p

Γ_n is proportional to v

$$\bar{\lambda}^2 \text{ proportional to } v^{-2} \Rightarrow \sigma_n \propto \frac{1}{v}$$

$$\Rightarrow \sigma_{wv} v \approx \text{const.} \approx \langle \sigma_{wv} v \rangle$$

reaction rate follows from (VI)

α -decay and fission

α decay Coulomb barrier is relatively low

$$(IV): 2\pi\gamma \approx 38 \quad \Delta Q \approx 1 \text{ MeV}$$



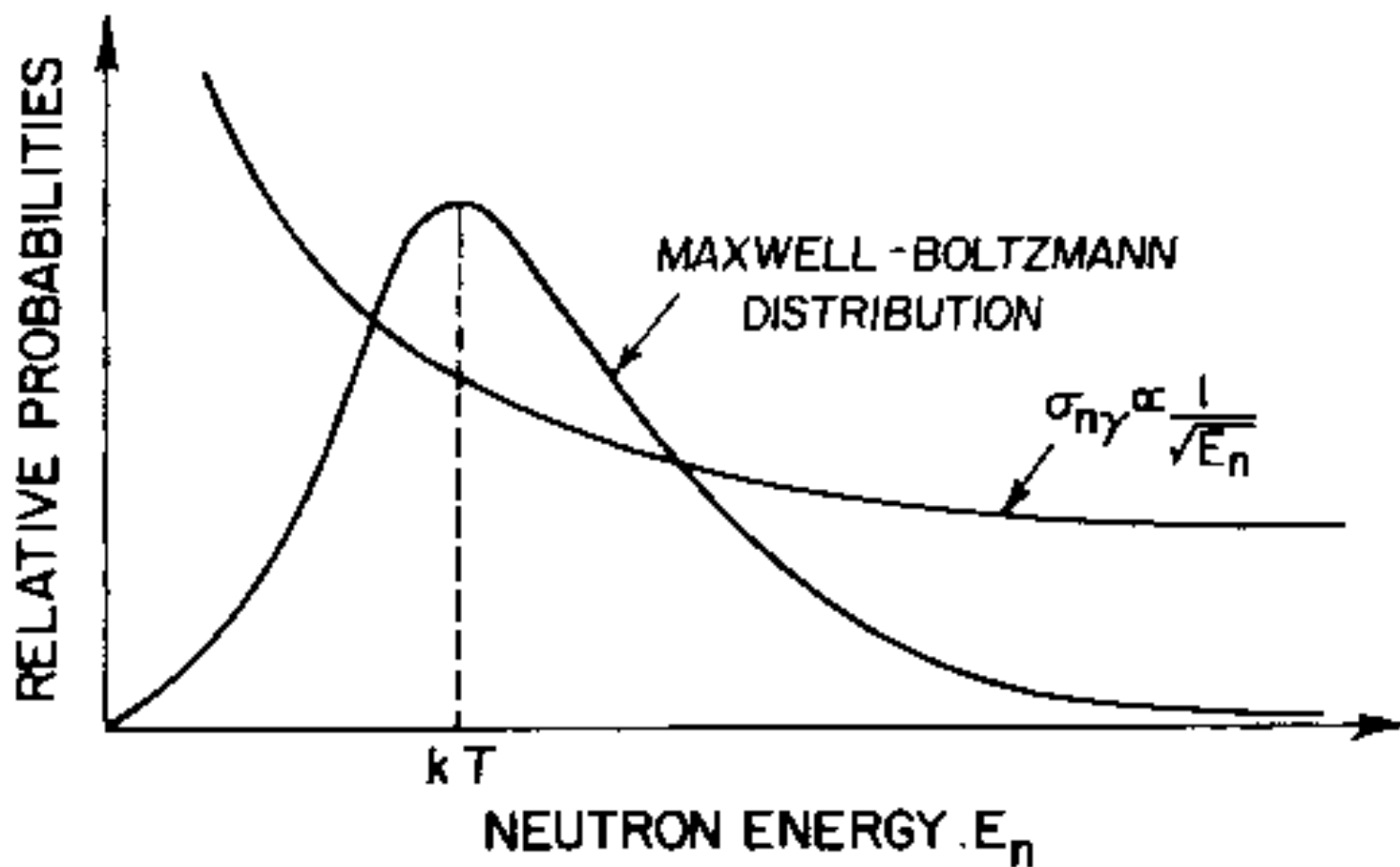


Fig. 2.13. Schematic superposition of the Maxwell energy distribution and neutron capture cross-section. The most probable energy for the capture process in stars is near kT . After Rolfs and Rodney (1988). Copyright by the University of Chicago. Courtesy Claus Rolfs.

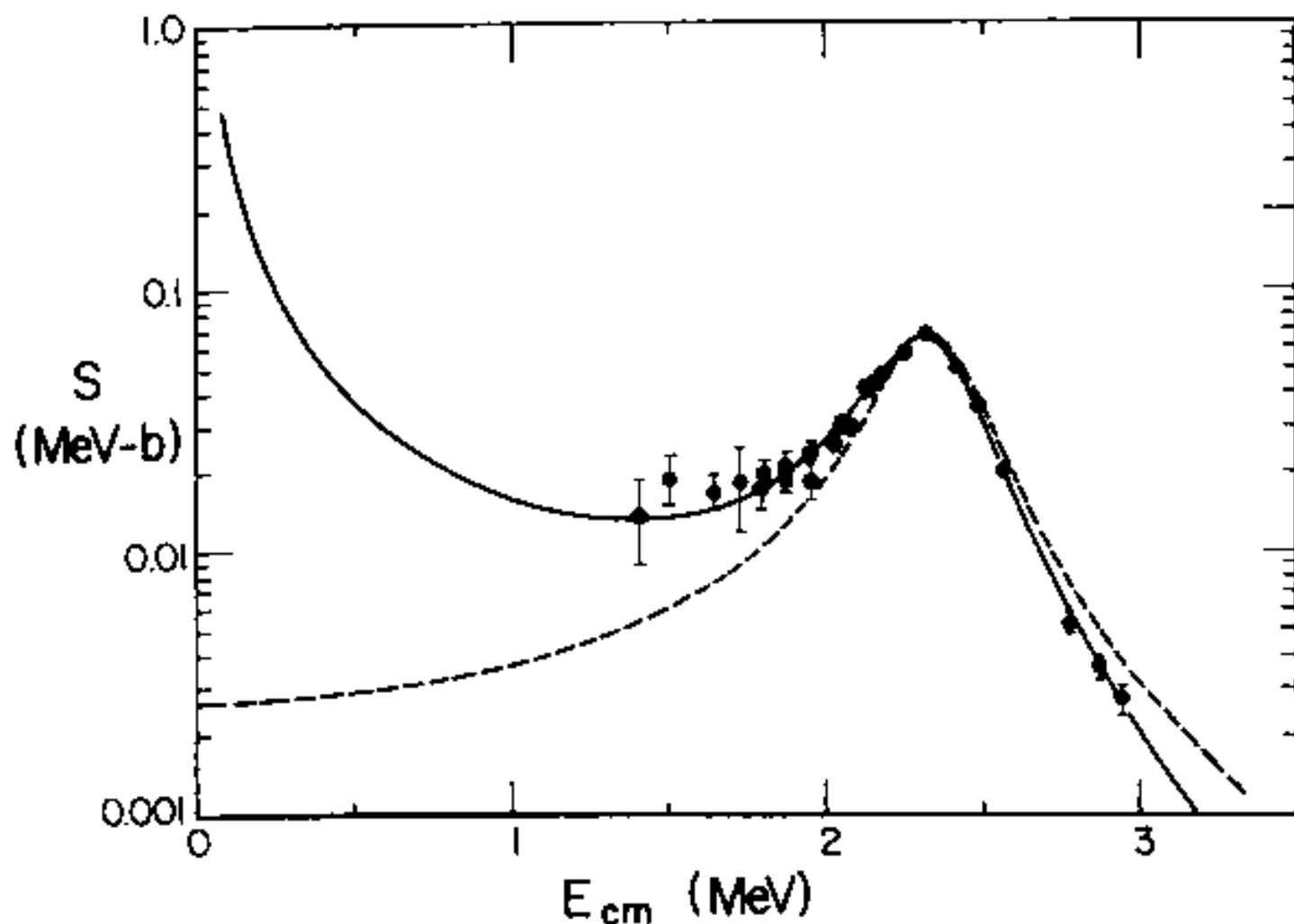


Fig. 2.12. S -factor for $^{12}\text{C}(\alpha, \gamma)^{16}\text{O}$. The dashed curve ignores the sub-threshold resonances, while the continuous curve allows for them, but the uncertainties are still significant at low energies. Koonin, Tombrello and Fox (1974). Reproduced with kind permission of Elsevier Science. Courtesy S. E. Koonin.